Volume 8:1-14

UJEMI+

The Undergraduate Journal of Experimental Microbiology & Immunology (+Peer Reviewed)

Examination into the HI-SEAS IV crew member microbiome reveals potential role of preferred interactions on skin microbial community structure

Kaya Frese, Bhavjot Naraina, Vanny Pornsinsiriruk, Arshia Shad

Department of Microbiology and Immunology, University of British Columbia, Vancouver, British Columbia, Canada

SUMMARY Astronauts experiencing prolonged space travel report increased skin hypersensitivity and delayed wound healing as a result of changes to the skin microbiome during space travel. In this study, we explored the effects of close social relationships within isolated built environments on the human skin microbiome. We analyzed the effect of crew interactions on the microbiome dynamics of six astronauts using a dataset from a year long Earth-bound Mars simulation called the Hawaii Space Exploration Analog and Simulation IV (HI-SEAS IV) mission. Microbial profiles were processed by Mahnert *et al.* based on amplicons targeting the V4 region of the 16S rRNA gene. We performed alpha and beta diversity longitudinal volatility analysis, taxonomic classifications, PCoA analysis, differential abundance analysis, and designed Venn diagrams to determine changes in microbiome dynamics. Within the dataset, we found that crew member pairs appeared to trend towards similar skin microbiomes, and microbiomes within pairs were found to be significantly more similar than between pairs. Furthermore, we found that the taxonomic composition of crew member skin microbiomes changed significantly between final and initial time points of the year-long mission. Our results suggest a potential for close physical interactions to modulate human skin microbiomes within isolated environments, and highlight the necessity for further examinations into the impact of such interactions on skin health.

INTRODUCTION

The skin microbiome is a major contributor to health and disease. The human skin is densely populated with bacteria, viruses, fungi, and arthropods (1). Together, these microorganisms make up the human skin microbiome, and host-microbiome interactions play a vital role in shaping host health. Many host-microbiome interactions are beneficial to the host, including calibration of tolerogenic immune responses, protection against pathogenic fungal and bacterial infections, and lipid metabolism (2). Conversely, dysregulation of the human skin microbiome is associated with disease, including recurring skin conditions such as atopic dermatitis and psoriasis (3). Dysbiosis of the skin microbiome has also been shown to increase susceptibility to more severe, acute infections by opportunistic bacteria such as *Staphylococcus aureus* and *Staphylococcus epidermidis* (4). While intrinsic factors such as age, sex, and body site can affect the human skin microbiome composition, extrinsic factors such as social relationships, built environment, and stress appear to play a disproportionate role in determining skin health (5, 6).

Published Online: September 2022

Citation: Frese K, Naraina B, Pornsinsiriruk V, and Shad A. 2022. Examination into the HI-SEAS IV crew member microbiome reveals potential role of preferred interactions on skin microbial community structure. UJEMI+ 8:1-14

Editor: Gara Dexter, University of British Columbia

Address correspondence to: Arshia Shad,

arshiashad@gmail.com

Social relationships, built environment and external stress factors impact the skin microbiome. As social animals, it is no surprise that interpersonal relationships impact the human skin microbiome. Families and couples that live together have been found to have significantly more similar gut and skin microbiomes compared to strangers (7, 8). Related to this, individuals and cohabitating groups that moved homes retained their microbial profile, as well as changing the microbial profile of their built environment (8). Built environment also impacts the human skin microbiome, and urban environments have been associated with decreased microbiome richness and evenness, and an increase in colonization by pathogenic fungal strains compared to rural environments (9). Psychological stress has also been implicated in detrimental skin microbiome changes and delayed wound healing (10, 11). Furthermore, isolated environments, such as those encountered in space travel, could potentially act as a unique model for the effect of prolonged interaction on skin microbiome community composition (12).

Space travel is a known model for the effects of social and environmental isolation on skin health. Space travel presents a major change in a person's social and environmental condition. Because microbial species are posited to be transferred through physical contact with humans, soil, local flora, and other environmental associations, as well as skin shedding, a severe decrease in social interactions could have a major effect on the skin microbiome of astronauts (8, 9). Furthermore, the extreme demands of space travel impose additional psychological stressors on astronauts. A 2019 study found that astronauts on the International Space Station (ISS) experienced significant changes in their skin microbiome over six to twelve months, with an overall increase in skin microbiome diversity, an increase in the abundance of pathogenic *Staphylococcus* and *Streptococcus* strains, and a decrease in beta- and gammaproteobacteria associated with protection from skin hypersensitivity (12). They also observed a greater incidence of skin rashes, validating several previous studies that also cited delayed wound healing and increased redness, itchiness, and bruising (13, 14). Another study published in 2021 analyzed microbial dynamics of crew members and the built environment of the Hawaii Space Exploration Analog and Simulation IV (HI-SEAS IV) mission, a year-long space travel simulation (15). Here, they confirmed an increase in overall skin microbiome diversity over time, a correlation between the microbiome of humans and their built environments, and significant differences in the microbiomes of various built environment surfaces (15).

While these studies elucidate a role for space travel in the alteration of human skin microbiome composition and resulting disease, we have identified a knowledge gap pertaining to the effect of close social relationships within isolated environments on the human skin microbiome. Over the course of the HI-SEAS IV mission, the six crew members self-reported their 'preferred interactions', or who they physically interacted with most closely. These self-reports formed three pairs of crew members. Using these pairs, we can study how close social relationships impact the human skin microbiome within isolated built environments. We hypothesize that similarity in skin microbial composition will be greater among the preferred interaction pairs, as previous findings have shown that coinhabitant shedding and direct contact is known to lead to an increase in similarity of the microbiome composition between individuals (16, 17).

METHODS AND MATERIALS

Dataset information. The HI-SEAS IV mission, operated by the University of Hawaii with funding from NASA, took place in an isolated dome on Mauna Loa, Hawaii, for one year from August 28, 2015 to August 28, 2016 (15). Six crew members (three male, three female) lived in the habitat with no outside contact, and outdoor activities were performed in a mock space suit. Resupply events occurred nine times, with contact delays and sanitation. Crew members showered one to three times per week, and the habitat was cleaned once per week. Wipes were taken from the skin of each crew member's torso every six weeks and stored at -20°C until the end of the isolation period, at which point they were shipped to Europe for analysis, where they were stored at -80°C (15). Analysis on these environmental and skin samples, such as DNA extraction, was carried out by Mahnert *et al.* (15). Mahnert *et al.* generated microbial profiles based on amplicons targeting the V4 region of the 16S rRNA gene and using the common primer pair F515-R806 with tags for Illumina sequencing (15).

Use of this primer pair allowed for coverage of most bacterial and some archaeal taxa (15). The raw amplicon data is available from the European Nucleotide Archive (accession number EMBL-EBI ERP118380). For any additional details regarding sample collection and analysis, refer to the paper generated by Mahnert *et al*. (15).

Sequence quality control. Demultiplexed sequences were imported into QIIME2, corrected for sequencing errors, truncated, and clustered into amplicon sequence variants (ASVs) using DADA2 (18, 19). The quality of HI-SEAS IV demultiplexed sequences remained fairly consistent until base pair 291, with mean Phred quality scores above thirty six throughout the sequence, indicating a base call certainty greater than 99.9% (20). Thus, the truncation length was set at base pair 291. Lastly, sequences were clustered into ASVs using DADA2. At the end of DADA2 denoising and clustering, a feature table was created as well as representative sequences.

Phylogenetic tree generation. A phylogenetic tree was generated to show evolutionary relationships between specimens for future diversity metrics such as Faith's phylogenetic diversity and UniFrac distance (18). FastTree 2 was used to align ASVs and assess base pair differences for the generation of representative sequences (21). This was further processed to produce phylogenetic trees based on relatedness (unrooted) and ancestral information (rooted) (18, 21).

Filtration of data. As we were only interested in the skin samples taken during isolation, the feature table was initially filtered, using QIIME2, to only include samples taken from the skin (18). This feature table was then further filtered, using the taxonomic classification of the ASVs, to exclude any mitochondrial sequences present, as our analysis focused on the presence of prokaryotic ASVs. To be able to deduce longitudinal changes in microbial diversity over the year-long isolation period, filtered feature tables were then generated based on collection time points. Although we initially planned to generate a filtered feature table for each individual collection time point, due to limited skin sample availability we had to group these collection time points into three sets of three, there being nine time points in total. Hence three filtered feature tables were generated, the first table covering days 0, 42, and 84, the second table covering days 126, 168, and 210, and the third table covering days 252, 294, and 336. These groupings represent early, middle, and late stages of the mission respectively.

Alpha rarefaction. Alpha rarefaction curves were generated in QIIME2 (18). Alpha rarefaction curves and the features table were used to determine a rarefaction depth of 15,720 reads per sample. This sequencing depth ensured retention of all six crew member skin microbiome samples at the initial and final collection time points while maximizing the number of ASVs maintained for proper statistical and taxonomic analysis.

Analysis of alpha and beta diversity. Alpha and beta diversity metrics were run using QIIME2 on the initial skin-filtered table, as well as the three time point-filtered feature tables (18). Shannon diversity and Pielou's evenness were selected as our alpha diversity metrics of interest, while weighted UniFrac distance was selected as our beta diversity metric of interest. The previously mentioned rarefaction depth of 15,720 reads per sample was chosen when running these metrics.

As part of this process, Kruskal-Wallis and pairwise PERMANOVA statistical tests were carried out to be able to observe any potentially significant differences in diversity between the skin microbiome of the crew members both as individuals, as well as within and between the preferred interaction pairs (22, 23). Kruskal-Wallis tests were performed for alpha diversity metrics and pairwise PERMANOVA tests were performed for beta diversity metrics.

Alpha and beta diversity longitudinal volatility analysis. The q2 longitudinal plugin in QIIME2 was utilized to run longitudinal volatility analysis on Shannon diversity, Pielou's evenness, and weighted UniFrac distance (24). Volatility analysis can be used to assess the

volatility of a dependent variable, in this case our alpha and beta diversity artifacts, over a continuous, independent variable, in this case time (24).

Taxonomic classification and taxa barplot generation. The Naïve Bayes classifier was used to predict the taxonomic affiliation of each representative sequence (25). This classifier was pre-trained with the Silva 138 99% OTUs to recognize the 515F/806R region of 16S rRNA gene (26). Taxonomic barplots were used to visualize the taxonomic composition of skin microbiomes from crew members (18).

PCoA and differential abundance analysis. R was used to generate PCoA plots based on weighted Unifrac distance and for differential abundance analysis between the initial and final collection time points (27). PCoA plots of the three time point-filtered tables were visualized based on the selected rarefaction depth of 15,720 reads per sample. Differential abundance analysis only included significant differences between initial and final collection time points ($p < 0.05$). R packages employed included tidyverse, vegan, ape, phyloseq, DESeq2, ggplot2, and ggthemes (28-34).

Venn diagrams. Shared and unique genera from taxa barplots were compared between crew members of preferred interaction pairs at the initial and final collection time point. These comparisons were used to illustrate Venn diagrams of preferred interaction pairs at the two time points.

RESULTS

Crew member skin microbiome diversity appeared to converge longitudinally but did not significantly change between time points. We first examined crew member skin microbiome alpha and beta diversity longitudinally. We found that Shannon diversity appeared to increase over time when examining all of our crew members (Fig. 1A). This highlights an apparent increase in skin microbiome diversity based on Shannon diversity which takes into account richness and abundance. However, there was no statistically significant difference by Shannon diversity between any of the time points (Kruskal-Wallis, $q > 0.05$). When looking at individual crew members, we noted the Shannon diversity appeared to increase for crew members 33, 35, and 36 over time (Fig. 1B). We also found that crew members seemed to converge towards more similar Shannon diversity values at the final collection time point (Fig. 1B). Convergence showed how their skin microbiome diversity appeared to become more similar with respect to Shannon diversity values towards the end of the isolation period.

Assessment of Pielou's evenness, a metric of community richness and evenness of the skin microbiome for all crew members together exhibited no discernable trend nor significant differences between the time points (Kruskal-Wallis, $q > 0.05$) (Fig. 1C). When looking at individual crew members we found that Pielou's evenness appeared to increase for crew members 33 and 36 over time, illustrating an apparent increase in skin microbiome diversity (Fig. 1D). We also noted an apparent convergence of crew members towards a similar Pielou's evenness value at the final collection time point (Fig. 1D). Convergence depicted how crew member skin microbiomes seemed to become more similar with respect to Pielou's Evenness values near the end of the isolation period, although these findings are not statistically significant.

We next examined the longitudinal volatility of axis 1 of our weighted UniFrac distance PCoA for all crew members and found no clear trend nor significant differences between time points (pairwise PERMANOVA, $q > 0.05$) (Fig. 1E). Examining individual crew members, we observed an upward trend for crew members 32, 35, and 36 (Fig. 1F). This highlighted an apparent relative change in crew member skin microbiome similarity as measured by weighted UniFrac distance PCoA which accounts for abundance and phylogenetic distance. We observed two points of convergence of weighted UniFrac distance on day 252 (Fig. 1F). Two groups of crew members 31, 34, and 35 and crew members 32, 33, and 36 respectively appeared to become similar (Fig. 1F). Convergence showed that the microbiome diversity of crew members within these two groups appeared to become more similar towards the end of the isolation period, however quantitative analysis did not support this observation.

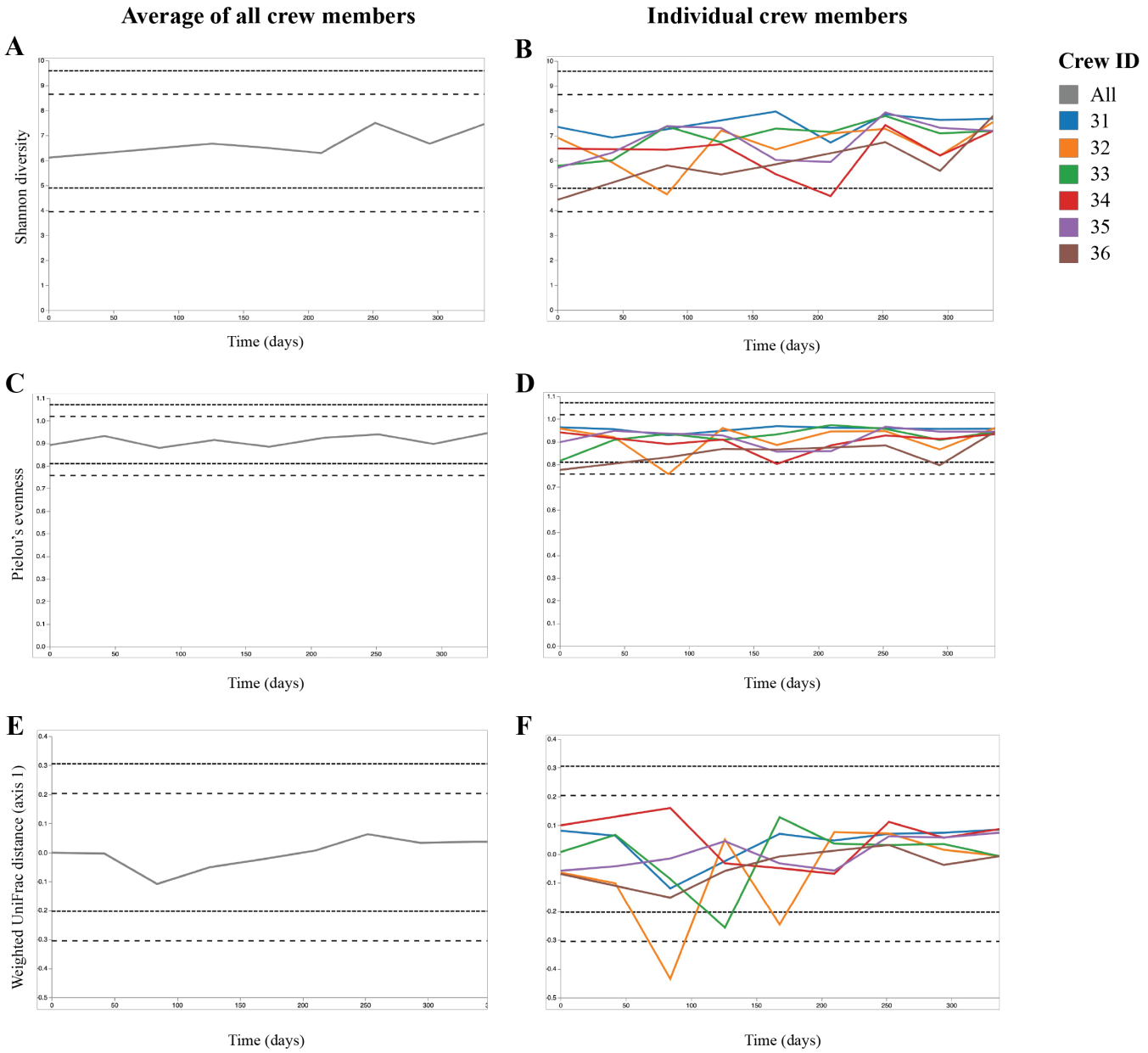

FIG. 1 Average crew skin microbiome diversity stays relatively constant longitudinally but individual analysis displays convergence trends. Longitudinal volatility analysis of Shannon diversity of (A) all crew members and (B) individual crew members. Longitudinal volatility analysis of Pielou's evenness of (C) all crew members and (D) individual crew members. Longitudinal volatility analysis along PCoA axis 1 (25.07%) based on weighted UniFrac distance of (E) all crew members and (F) individual crew members. Fig. 1F is parsed out in Fig. 3 as pairs. No significant difference was observed between time points for all crew members (Kruskal-Wallis, pairwise PERMANOVA, $q > 0.05$) (A, C, E).

Preferred interaction patterns had a significant impact on skin microbial diversity. Considering the aforementioned convergence patterns that were observed in crew member skin microbiome diversity, we were interested in whether preferred interaction between crew members had an impact on any potential convergence. Hence, we then examined the potential influence of preferred interaction between certain crew members on the development of similarities or differences in microbial diversity over the isolation period. The first step in this preferred interaction analysis was to look within these interaction pairs and compare one crew

member to the other. To this end, we carried out weighted UniFrac distance beta diversity analysis, and once again used axis 1 of the weighted UniFrac distance PCoA to generate longitudinal volatility plots, one for each preferred interaction pair (Fig. 2A-C). For preferred interaction pair 31-34, weighted UniFrac distances initially fluctuated without a discernible pattern, but then seemed to converge beginning on day 252 of the isolation period,

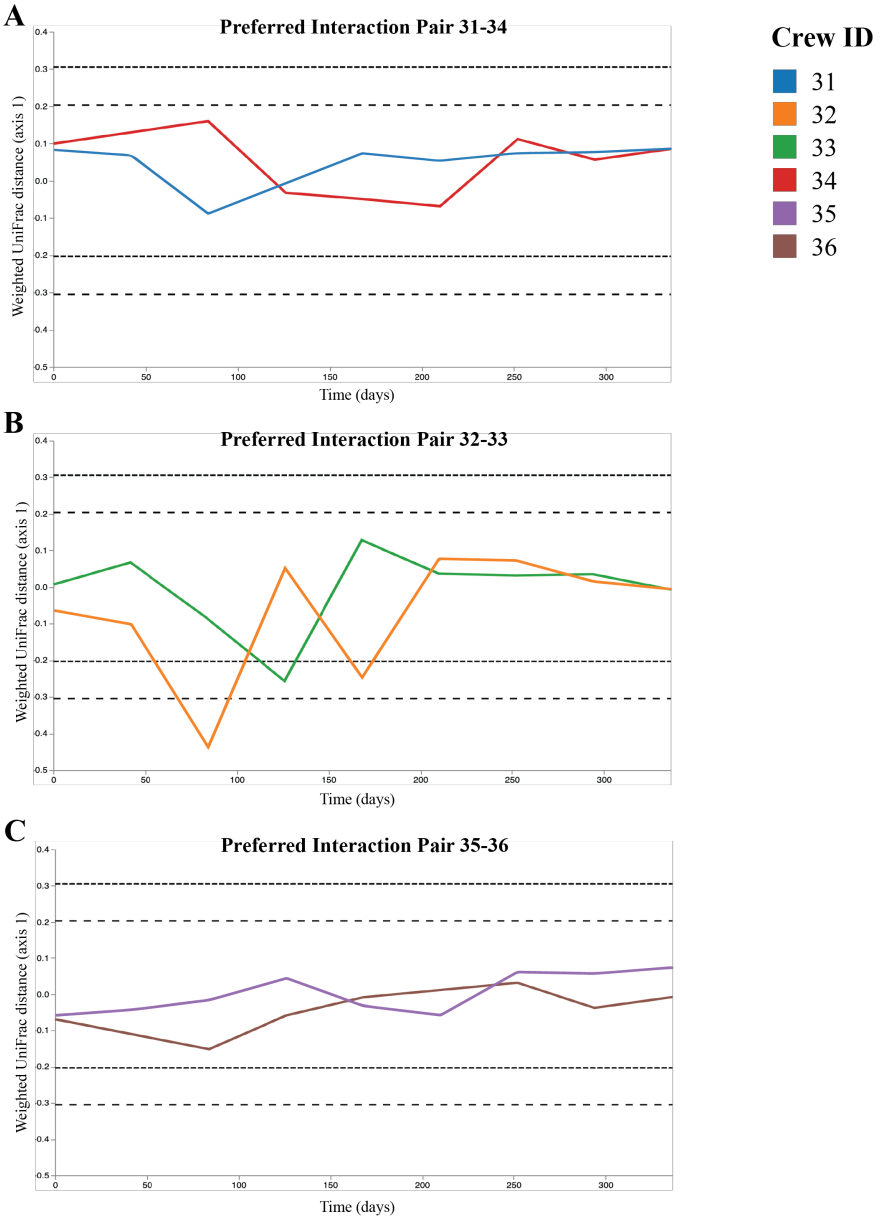

FIG. 2 Longitudinal analysis within preferred interaction pairs displays patterns of convergence for two out of three pairs. Longitudinal volatility analysis along PCoA axis 1 (25.07%) based on weighted UniFrac distance for preferred interaction pairs (A) 31-34, (B) 32-33, and (C) 35-36. Fig. 3 shows Fig. 1F parsed out into pairs.

overlapping by the end of isolation (Fig. 2A). This trend pointed to these two crew members potentially becoming more similar with regards to skin microbiome diversity over time. For pair 32-33, a similar pattern was observed. The weighted UniFrac distances had the same initial fluctuation, this time appearing to converge on day 210 of the isolation period, once again overlapping by the end of isolation (Fig. 2B). Preferred interaction pair 32-33 also appeared to grow more similar in skin microbiome diversity over time. For pair 35-36 however, there was no pattern of convergence (Fig. 2C). In fact, weighted UniFrac distances for crew members 35 and 36 appear closer to each other at the beginning of isolation than they were at the end (Fig. 2C).

After within-pair comparison, we compared microbial diversity between these preferred interaction pairs. It was important to do so as analyzing microbial diversity both within and between these pairs allowed us to understand what impact preferred interaction would be

having on microbiome composition. For this purpose, another weighted UniFrac distance longitudinal volatility plot was generated, separated based on preferred interaction pairs (Fig. 3A). Based on this longitudinal analysis, the only noticeable trend was that of pair 31-34 growing more similar in microbiome diversity to the other two pairs, 32-33 and 35-36 (Fig. 3A).

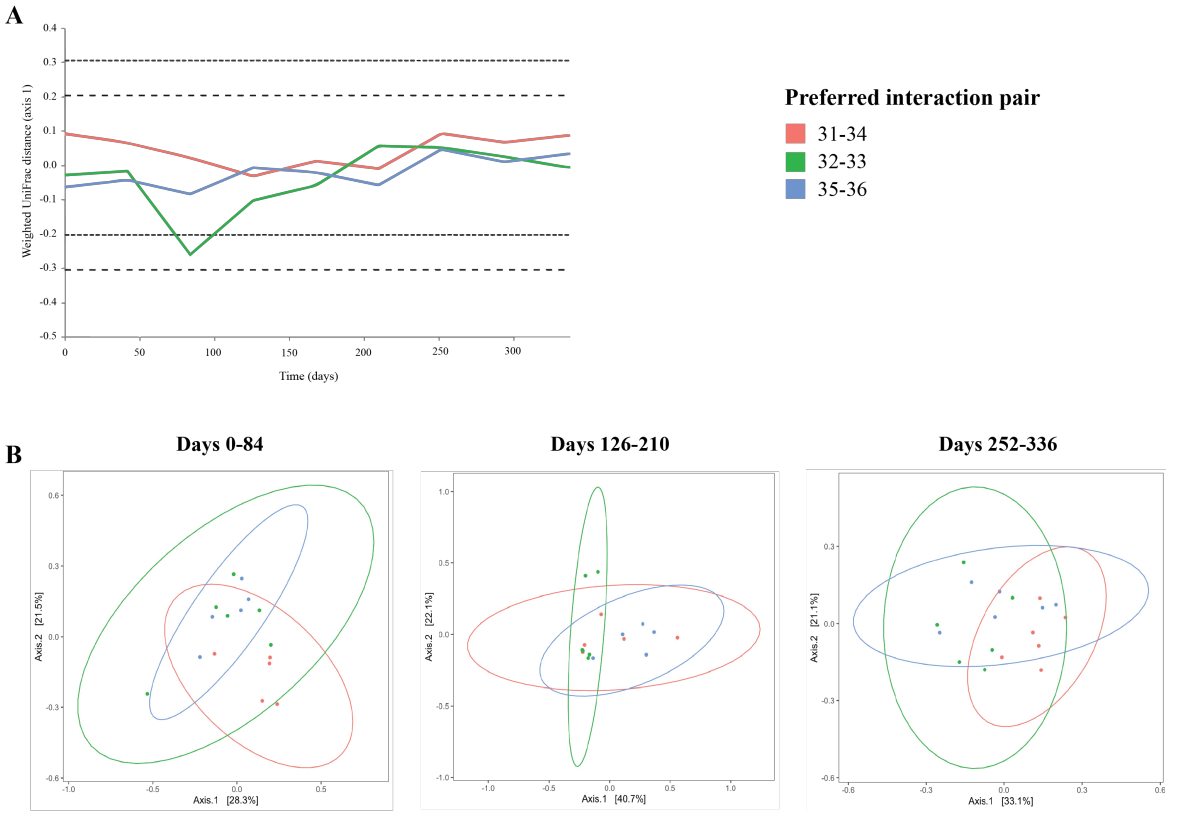

FIG. 3 Longitudinal analysis between preferred interaction pairs shows significant differences between some pairs. (A) Longitudinal volatility analysis along PCoA axis 1 (25.07%) based on weighted UniFrac distance for all preferred interaction pairs. (B) Weighted UniFrac distance PCoA plots for the three filtered time points where pairs are separated by eclipses. Significant differences exist between preferred interaction pairs 31-34 and 35-36 for days 0-84 (pairwise PERMANOVA, q = 0.021) and between pairs 31-34 and 32-33 for days 252-336 (pairwise PERMANOVA, q = 0.012).

The next step was to test for significant differences between the interaction pairs via beta diversity analysis. As mentioned previously, the collection time points were grouped into three sets of three: days 0-84, 126-210, and 252-336. The weighted UniFrac distance analysis returned two significant results. Firstly, for the time point group covering days 0-84, weighted UniFrac distances were significantly different between pair 31-34 and pair 35-36 (pairwise PERMANOVA, q = 0.021) (Fig. 3B). Secondly, for the time point group covering days 252-336, weighted UniFrac distances were found to be significantly different between pairs 31-34 and 32-33 (pairwise PERMANOVA, q = 0.012) (Fig. 3B). There were no significant differences between any of the pairs for the time point group covering days 126-210 (Fig. 3B). As a note, when we removed the longitudinal aspect of our analysis and instead ran weighted UniFrac distance diversity analysis on all collection time points combined, pair 31-34 was found to be significantly different from both pair 32-33 (pairwise PERMANOVA, q = 0.009), and pair 35-36 (pairwise PERMANOVA, q = 0.009) (Supplemental Fig. 3).

Taxonomic composition of preferred interaction pairs varied between the start and end of the isolation period. The taxonomic composition of preferred interaction pairs was assessed at the initial and final collection time point via taxonomic barplots to further examine

the differences in diversity that were observed longitudinally. Comparison of these barplots suggest an increased similarity in taxonomic composition between all crew members at the final relative to the initial collection time point (Supplemental Fig. 1). This seems to reflect the apparent trend towards homogeneity observed in the longitudinal analysis (Fig. 1). Based on the taxonomic analysis, Venn diagrams were generated to represent the number of unique and shared taxa at the genus level within preferred interaction pairs at the start and end of the isolation period (Fig. 4). Pairs 31-34 and 32-33 showed minor changes in the number of shared taxa at the final relative to the initial collection time point, +1 and -2 respectively. In comparison, we observed an increase of 24 shared taxonomic genera for pair 35-36. Notably, there was a considerable shift between the initial and final collection time point regarding the number of taxa unique to one crew member within each pair. A decrease in phylogenetic diversity of crew members 31 and 33 was observed by the final collection time point, where genera unique to each member decreased by 26 and 42 respectively. Contrastingly, crew members 32, 34, 35, and 36 showed an increase in the number of unique genera by 3, 26, 4, and 46 respectively (Fig. 4).

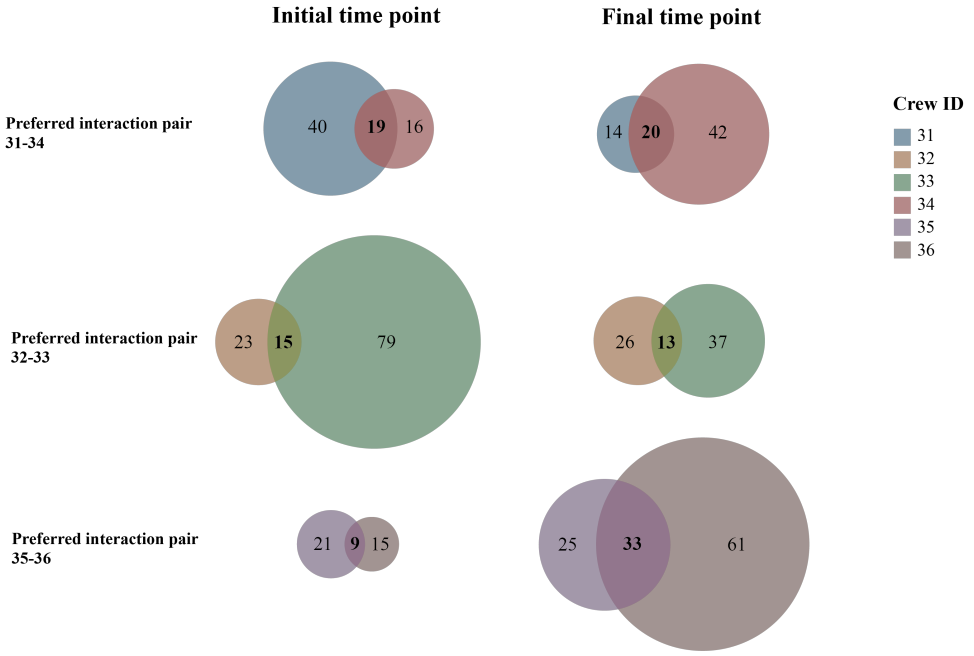

FIG. 4 Taxonomic composition of preferred interaction pairs varies between the start and end of the isolation period. Venn diagrams represent the number of unique and shared taxa at the genus level within preferred interaction pairs at the start and end of the isolation period.

To identify the skin microbiome taxa significantly associated with prolonged isolation, differential abundance analysis at the genus level of all crew members was performed. Abundance was derived by comparison of the final relative to the initial collection time point. Differential abundance analysis identified eight microbial genera that were significantly more abundant at the final relative to the initial collection time point in the cohort's skin microbiome: *WPS-2*, *Vulcaniibacterium*, *Blastomonas*, *Cloacibacterium*, *Thermaerobacter*, *Verticiella*, *Bacteriap25*, and *Nitrosopumilaceae* ($p<0.05$). In comparison, six microbial genera were identified as significantly less abundant: *Clostridium sensu stricto 13, Lysinibacillus, Devosia, Blautia, Modestobacter,* and *Massilia* (Supplemental Fig. 2) ($p<0.05$).

DISCUSSION

Longitudinal changes in crew member microbiome diversity corroborates previous findings and seems to illustrate convergence towards the end of the isolation period. Our first avenue of exploration was to examine how crew member skin microbiome diversity changed over time in the HI-SEAS IV isolated environment. We found that skin microbiome diversity when taking into consideration both alpha diversity metrics, Shannon diversity and Pielou's evenness, as well as beta diversity metrics with weighted UniFrac distance, did not exhibit significant differences longitudinally (Fig. 1A-F). However, we observed the trend that Shannon diversity appeared to increase throughout the isolation period. This apparent

trend affirms a prior study using HI-SEAS IV mission data which found that skin crew microbiome diversity increased throughout the isolation period with respect to Shannon diversity (15). This also seems to corroborate a study of the astronauts on the ISS that identified an increase in overall skin microbiome diversity (12). An increase in skin microbiome diversity could be resulting from direct physical contact and shedding of microorganisms of the crew within the confined environment (16, 17). Confounding variables could be influencing this apparent increase in skin microbiome diversity, through potential introduction of microorganisms through resupply events and their associated addition of fermented products, and simulated Martian walks on Mauna Loa with mock spacesuits (15, 35).

We also noticed that this apparent increase in microbiome diversity is only discernible with Shannon diversity and not with Pielou's evenness (Fig. 1A, C, E). This could suggest that the trend is only visible when we do not account for evenness. Thus, the evenness which accounts for relative abundance of the skin microbiome might be more similar amongst the crew members than abundance longitudinally. The presence of rare ASVs could potentially be a factor in driving these differences, especially considering we did not filter rare ASVs out of the dataset prior to analysis. The reasoning for this choice is explained further in limitations.

Additionally, we noted convergence of both alpha diversity metrics with Shannon diversity and Pielou's evenness values appearing to become more similar between the crew by the end of the isolation period (Fig. 1B, D, F). We also noted trends of convergence between two groups of crew members with 31, 34, and 35 converging together and separately from 32, 33, and 36. As described in the previous section, these observed convergences could be explained by direct physical contact and shedding of microbes between crew members leading to homogenization of their skin microbiomes (16, 17). The convergence with alpha diversity metrics was only observed at the final collection time point making it more difficult to conclusively determine a trend. However, the bimodal convergence pattern with PCoA axis 1 based on weighted UniFrac distance became apparent earlier in the isolation period at day 252 lending more credibility to this trend. This bimodal pattern of convergence could reflect potential differences in the two groups of crew members in terms of crew interaction as well as confounding variables such as hygiene practices and spatial preferences within the isolated environment (15). Changes in skin microbiome is a crucial consideration in space exploration because a decrease in diversity has been associated with dysbiosis and correlated skin diseases which would require predetermined planning to manage prior to leaving Earth (1, 4, 12).

Observed significance of preferred interaction on changes in skin microbial diversity points to the impact of the personal bubble. Our analysis of preferred interaction patterns in the HI-SEAS IV study returned interesting results regarding the impact of such patterns on the diversity of crew member skin microbiomes. Our longitudinal analysis highlighted significant differences both between preferred interaction pairs 31-34 and 32-33, as well as between pairs 31-34 and 35-36, albeit within different time point groups (Fig. 3B). Further, our overall weighted UniFrac distance analysis, accounting for all skin samples collected during the isolation period, found significant differences between preferred interaction pair 31-34 and both other pairs 32-33 and 35-36 (Supplemental Fig. 3). When looking within these pairs however, no significant difference was observed between the crew members. These findings point to the potential effect that close physical interaction and social circles may have on the development of the human skin microbiome.

Previous research has found that cohabitation and close social relationships are often positively correlated with a similarity in the diversity and composition of the microbiome (16, 17). One study even observed that cohabitating humans and their pet dog all exhibited shared microbiota (17). Our analysis of the relationship between preferred interaction and the skin microbiome of the HI-SEAS IV crew members appears to be exhibiting an analogous correlation. It seems then, that even in an isolated environment such as the HI-SEAS IV dome, physical interaction patterns could play a part in skin microbiome diversity and composition. Even though all the crew members were cohabiting the same isolated environment, pairs that interacted most frequently appear to show greater similarity in their skin microbiota compared to the other pairs. Perhaps the same concept would apply to space exploration missions. Space flight vessels and planetary habitats are isolated environments, and although further research

into this topic is necessary, our findings may be providing a potential avenue to explore in regard to the developmental patterns of astronaut skin microbiomes during future manned spaceflight and colonization efforts.

Taxonomic analysis shows a lack of noticeable increase in shared microbial taxa within preferred interaction pairs. Based on the more even distribution at final relative to initial time point by taxonomic barplots (Supplemental Fig. 1), and the patterns of convergence observed within pairs (Fig. 2A, B), we expected a trend towards taxonomic homogeneity within the preferred interaction pairs. Despite these observations, an increase in shared genera was only observed within pair 35-36 (Fig. 4), which unexpectedly was also the pair that appeared to show no pattern of convergence (Fig. 2C). This contradiction suggests a lack of correlation between close physical interaction and phylogenetic affiliation at the genus level. That being said, individual crew members, including 36, showed considerable change in phylogenetic diversity at the final relative to initial time point. The number of genera unique to each member within pairs changed in either direction by as much as -42 and +46 (Fig. 4). Thus, while there are substantial changes in microbiome composition within an isolated environment, there seems to be no consistent pattern of increase or decrease in taxonomic diversity. This could be explained by the impacts of confounding or lurking variables that we do not consider in our analysis including weekly general cleaning, time of shower relative to sampling, and the introduction of microorganisms by fermented products (15). It would be important to perform multiple longitudinal analyses against those variables measured by Mahnert *et al.* (15) to identify which, if any, significantly impact taxonomic composition. By doing so, space travel can be optimized to select for microbes that are beneficial to hosts and against those that could be detrimental.

Differential abundance analysis comparing initial and final time points showed several enriched and suppressed genera within crew member skin microbiomes (Supplemental Fig. 2). Suppressed genera included *Blautia*, *Lysinibacillus*, and *Massilia*. *Lysinibacillus* have known antifungal capabilities, while *Blautia* depletion is correlated to rosacea, an chronic inflammatory skin condition (36, 37). Notably, *Massilia* belong to the betaproteobacteria, which the 2019 study on the ISS also reported to be suppressed (12). Beta- and gammaproteobacteria, including *Massilia* and *Blautia*, are abundant in the soil, which may explain their suppression in space travel and space travel simulations (38, 39). Enriched genera included *Blastomonas* and *Cloacibacterium*, which are associated with antibiotic resistance and untreated wastewater respectively (40, 41). Interestingly, enriched genera also included *Thermaerobacter*, and *Bacteriap25*, genera associated with deep ocean sediments (42, 43). Furthermore, the archaeon *Nitrosopumilaceae* was enriched, which does not generally colonize humans (44).

Limitations A few important limitations exist in our analysis, largely due to the data collection process during the HI-SEAS IV study by Mahnert *et al.* (15). With regard to the collection of skin wipes, there were no replicates collected per time point (15). This meant that only one skin sample was collected from each crew member per collection time point, which made us unable to run the beta diversity metrics for each time point due to lack of sufficient skin samples. This, as mentioned previously, was the reason our time point analysis was done in three groups of three, rather than per collection time point. Further, skin wipes were only collected from the torso. It has been shown that the composition of the skin microbiome can vary significantly from one body site to the next (1). Hence, specifying the exact torso location, sampling from more body sites, and increasing the limited sample size may have proven insightful.

Moreover, the concept of ‘preferred interaction’ is not clearly defined beyond the fact that the pairings were based on self-reported interaction patterns between the crew members (15). There was no mention of the types of activities the crew members within the pairs shared with one another, or how often they interacted with each other as opposed to the other participants. Moreover, the metadata category for preferred interaction pairs only consisted of combining the individual crew member skin samples into that of a pair. Perhaps the addition of a skin sample type taken after the pairs physically interacted, for instance after a handshake or a hug, could have introduced novel data for downstream analysis.

Furthermore, we chose not to filter for rare ASVs in our analysis pipeline in order not to lose certain significant but rare ASVs. However, this would come with the caveat of potential sequencing errors having been included in the overall analysis. We still believed that the pros outweighed the cons in this scenario, as we lost a significant amount (~40%) of ASVs if we did filter for rare (0.005%) ASVs, but it is important to make mention of it as a potential limitation.

Lastly, other confounding variables including the impact of the environment or lifestyle were not considered. For example, no record was taken in regard to the use of any potential antibiotics or probiotics by the HI-SEAS IV crew members. Such compounds could introduce significant changes in microbiota composition, and could act as confounding variables when it comes to the analysis of the human microbiome (45).

Conclusions Our study aimed to assess the impact of prolonged environmental isolation and preferred interaction patterns on the diversity and composition of the skin microbiome over time within the HI-SEAS IV mission. We first examined the change of crew member skin microbiome diversity within the isolated environment and found that it appeared to trend towards homogeneity over time. However, there was no significant difference in diversity between collection time points, potentially limiting the credibility of this trend. Next, we examined the impact of preferred interactions on skin microbiome diversity where we observed significant differences between preferred pairs, but not within. Our findings point to the possible effect that preferred interactions might have on the trajectory of skin microbiome evolution. Finally, we examined taxonomic composition comparing the final to the initial collection time point accounting for preferred interactions. Our results suggest differences in taxonomic composition and a lack of noticeable increase in shared microbial taxa between the two time points. Our findings provide a foundation for future examinations of skin microbiome structure and function within isolated environments in the context of space exploration.

Future Directions To further characterize skin microbiome changes in isolation, future studies should examine taxonomy and diversity metrics in post-isolation skin samples which were collected at day 400. Our results showed a convergence in diversity within pairs 31-34 and 32-33 (Fig. 2A, B). As such, divergence at day 400 would support that social relationships and built environments have significant impacts on microbial diversity. Comparison of compositional changes during and after isolation would provide valuable information about whether these changes from isolation are temporary or sustained. Moreover, it could offer insight into how the skin microbiome of an astronaut changes after they return to Earth which has further implications on individual and community health.

To better define the impact of preferred interactions on diversity and taxonomic composition, it would be worthwhile to assess the relative contribution of different variables on the changes we observe in diversity. For example, preliminary analysis of PCoA by phenotype (data not shown) showed clustering patterns suggestive of some impact on diversity. Given samples were collected by wipes from the torso, shower duration and timing likely also contribute to longitudinal changes in diversity. As such, future studies could explore or control for the effect of other variables on diversity metrics. This could allow for better understanding of the interaction between different variables and their cumulative impact on diversity in an isolated environment. Moreover, it would address gaps in knowledge from our analysis that would be necessary to select for and against microbial species to ensure host health in space travel.

Future studies could build upon our investigation by performing further differential abundance analysis and literature reviews to characterize the skin microbiome of a general population. An initial look into differential abundance analysis revealed several genera that were significantly enriched or suppressed within crew member skin microbiomes at the final relative to the initial time point (Supplemental Fig. 2). Future studies could perform differential abundance analysis between sequential timepoints to identify when major microbial taxa were introduced to the environment. This could have significant implications

on host health in space travel given we observed suppression of *Blautia* and enrichment of *Blastomonas*, which are associated with a chronic skin inflammatory condition and antibiotic resistance respectively (37, 40). Given the potential health implications this could have on astronauts, it could be important to assess how representative our cohort is of a general population. A literature review of the typical skin microbiome composition could offer insight into the generalizability of our findings.

Another path future studies could take when building upon our differential abundance analysis is through functional profiling of the skin microbiome. Understanding how certain functional niches are filled by microbes in an isolated environment, such as HI-SEAS IV, could prove invaluable in selecting for beneficial microbes in future manned spaceflight missions.

ACKNOWLEDGEMENTS

We would like to thank the Department of Microbiology and Immunology at the University of British Columbia for providing the resources and funding required to complete this study. We would also like to thank the MICB 447 teaching team (Evelyn Sun, Steven Hallam, Stephan Koenig, Stefanie Sternagel, and Zakhar Krekhno) for providing instruction, guidance, and technical support. As well, we wish to thank our peers (Adrian Chen, Immanuel Abdi, Jessica Shen, Kevin Xiao, Aneesa Khan, Garshana Rajkumar, John Park, Kitty Martens, Nemat Haroon, Jaskirat Malhi, and Ali Anwari) for their feedback on our study. We would also like to thank Diane Li, Kyle Ching, and Wesley J. Hunt for the technical support their publication on the HI-SEAS IV dataset provided. Finally, we would like to thank the NASA Human Research Program for funding and organizing the HI-SEAS IV mission. We would also like to thank two anonymous reviewers for constructive feedback on this manuscript.

CONTRIBUTIONS

Kaya Frese: Contributed to the analysis of alpha and beta diversity and composed Future Directions, as well as parts of Methods, Results, Discussion, and figure captions.
Bhavjot Naraina: Contributed to the analysis of alpha and beta diversity and composed Conclusion, as well as parts of Methods, Results, Discussion, and figure captions.
Vanny Pornsinsiriruk: Generated the manuscript figures and composed the Abstract, Introduction, and parts of Methods and Discussion.
Arshia Shad: Contributed to the analysis of alpha and beta diversity and composed Limitations, as well as parts of Methods, Results, Discussion, and figure captions.
Co-authorship credit should be considered equal for all authors.

REFERENCES

1. **Byrd AL, Belkaid Y, Segre JA**. 2018. The human skin microbiome. *Nat Rev Microbiol*. **16**(3):143-155.
2. **Schommer NN, Gallo RL**. 2013. Structure and function of the human skin microbiome. *Trends Microbiol*. **21**(12):660-668.
3. **Weyrich LS, Dixit S, Farrer AG, Cooper AJ, Cooper AJ**. 2015. The skin microbiome: Associations between altered microbial communities and disease. *Australas J Dermatol*. **56**(4):268-274.
4. **Grice EA, Segre JA**. 2011. The skin microbiome. *Nat Rev Microbiol*. **9**(4):244-253.
5. **Dimitriu PA, Iker B, Malik K, Leung H, Mohn WW, Hillebrand GG**. 2019. New Insights into the Intrinsic and Extrinsic Factors That Shape the Human Skin Microbiome. *mBio*. **10**(4):e00839-19.
6. **Grice EA, Kong HH, Conlan S, Deming CB, Davis J, Young AC; NISC Comparative Sequencing Program, Bouffard GG, Blakesley RW, Murray PR, Green ED, Turner ML, Segre JA**. 2009. Topographical and temporal diversity of the human skin microbiome. *Science*. **324**(5931):1190-1192.
7. **Ross AA, Doxey AC, Neufeld JD**. 2017. The Skin Microbiome of Cohabiting Couples. *mSystems*. **2**(4):e00043-17.
8. **Lax S, Smith DP, Hampton-Marcell J, Owens SM, Handley KM, Scott NM, Gibbons SM, Larsen P, Shogan BD, Weiss S, Metcalf JL, Ursell LK, Vázquez-Baeza Y, Van Treuren W, Hasan NA, Gibson MK, Colwell R, Dantas G, Knight R, Gilbert JA**. 2014. Longitudinal analysis of microbial interaction between humans and the indoor environment. *Science*. **345**(6200):1048-1052.

9. **Callewaert C, Ravard Helffer K, Lebaron P**. 2020. Skin Microbiome and its Interplay with the Environment. *Am J Clin Dermatol*. **21**(Suppl 1):4-11.
10. **Prescott SL, Larcombe DL, Logan AC, West C, Burks W, Caraballo L, Levin M, Etten EV, Horwitz P, Kozyrskyj A, Campbell DE**. 2017. The skin microbiome: impact of modern environments on skin ecology, barrier integrity, and systemic immune programming. *World Allergy Organ J*. **10**(1):29.
11. **Holmes CJ, Plichta JK, Gamelli RL, Radek KA**. 2015. Dynamic Role of Host Stress Responses in Modulating the Cutaneous Microbiome: Implications for Wound Healing and Infection. *Adv Wound Care*. **4**(1):24-37.
12. **Voorhies AA, Mark Ott C, Mehta S, Pierson DL, Crucian BE, Feiveson A, Oubre CM, Torralba M, Moncera K, Zhang Y, Zurek E, Lorenzi HA**. 2019. Study of the impact of long-duration space missions at the International Space Station on the astronaut microbiome. *Sci Rep*. **9**(1):9911.
13. **Braun N, Thomas S, Tronnier H, Heinrich U**. 2019. Self-Reported Skin Changes by a Selected Number of Astronauts after Long-Duration Mission on ISS as Part of the Skin B Project. *Skin Pharmacol Physiol*. **32**(1):52-57.
14. **Crucian B, Babiak-Vazquez A, Johnston S, Pierson DL, Ott CM, Sams C**. 2016. Incidence of clinical symptoms during long-duration orbital spaceflight. *Int J Gen Med*. **9**:383-391.
15. **Mahnert A, Verseux C, Schwendner P, Koskinen K, Kumpitsch C, Blohs M, Wink L, Brunner D, Goessler T, Billi D, Moissl-Eichinger C**. 2021. Microbiome dynamics during the HI-SEAS IV mission, and implications for future crewed missions beyond Earth. *Microbiome*. **9**(1):27.
16. **Dill-McFarland KA, Tang Z-Z, Kemis JH, Kerby RL, Chen G, Palloni A, Sorenson T, Rey FE, Herd P.** 2019. Close social relationships correlate with human gut microbiota composition. *Scientific Reports.* **9**:703.
17. **Song SJ, Lauber C, Costello EK, Lozupone CA, Humphrey G, Berg-Lyons D, Caporaso JG, Knights D, Clemente JC, Nakielny S, Gordon JI, Fierer N, Knight R.** 2013. Cohabiting family members share microbiota with one another and with their dogs. *eLife.* **2**:e00458.
18. **Bolyen E, Rideout JR, Dillon MR, Bokulich NA, Abnet CC, Al-Ghalith GA, Alexander H, Alm EJ, Arumugam M, Asnicar F, Bai Y, Bisanz JE, Bittinger K, Brejnrod A, Brislawn CJ, Brown CT, Callahan BJ, Caraballo-Rodríguez AM, Chase J, Cope EK, Da Silva R, Diener C, Dorrestein PC, Douglas GM, Durall DM, Duvallet C, Edwardson CF, Ernst M, Estaki M, Fouquier J, Gauglitz JM, Gibbons SM, Gibson DL, Gonzalez A, Gorlick K, Guo J, Hillmann B, Holmes S, Holste H, Huttenhower C, Huttley GA, Janssen S, Jarmusch AK, Jiang L, Kaehler BD, Kang KB, Keefe CR, Keim P, Kelley ST, Knights D, Koester I, Kosciolek T, Kreps J, Langille MGI, Lee J, Ley R, Liu YX, Loftfield E, Lozupone C, Maher M, Marotz C, Martin BD, McDonald D, McIver LJ, Melnik AV, Metcalf JL, Morgan SC, Morton JT, Naimey AT, Navas-Molina JA, Nothias LF, Orchanian SB, Pearson T, Peoples SL, Petras D, Preuss ML, Pruesse E, Rasmussen LB, Rivers A, Robeson MS 2nd, Rosenthal P, Segata N, Shaffer M, Shiffer A, Sinha R, Song SJ, Spear JR, Swafford AD, Thompson LR, Torres PJ, Trinh P, Tripathi A, Turnbaugh PJ, Ul-Hasan S, van der Hooft JJJ, Vargas F, Vázquez-Baeza Y, Vogtmann E, von Hippel M, Walters W, Wan Y, Wang M, Warren J, Weber KC, Williamson CHD, Willis AD, Xu ZZ, Zaneveld JR, Zhang Y, Zhu Q, Knight R, Caporaso JG**. 2019. Reproducible, interactive, scalable, and extensible microbiome data science using QIIME2. *Nat. Biotechnol*. **37**:852-857.
19. **Callahan BJ, McMurdie PJ, Rosen MJ, Han AW, Johnson AJ, Holmes SP**. 2016. DADA2: High resolution sample inference from Illumina amplicon data. *Nat. Methods.* **13**(7):581-583.
20. **Liao P, Satten GA, Hu YJ.** 2017. PhredEM: a phred-score-informed genotype-calling approach for next-generation sequencing studies. *Genet Epidemiol*. **41**(5):375-387.
21. **Price MN, Dehal PS, Arkin AP.** 2010. FastTree 2 – Approximately Maximum-Likelihood Trees for Large Alignments. *PLoS One.* b:e9490.
22. **Kruskal WH, Wallis WA.** 1952. Use of ranks in one-criterion variance analysis. *J Am Stat Assoc.* **47**:583–621.
23. **Anderson MJ.** 2001. A new method for non-parametric multivariate analysis of variance. *Austral Ecol.* **26**:32–46.
24. **Bokulich NA, Dillon MR, Zhang Y, Rideout JR, Bolyen E, Li H, Albert PS, Caporaso JG.** 2018. q2-longitudinal : longitudinal and paired-sample analyses of microbiome data. *mSystems*. **3**:1–9.
25. **Bokulich NA, Kaehler BD, Rideout JR, Dillon M, Bolyen E, Knight R, Huttley GA, Gregory Caporaso J.** 2018. Optimizing taxonomic classification of marker-gene amplicon sequences with QIIME 2's Q2-feature-classifier plugin. *Microbiome.* **6**:90.
26. **Quast C, Pruesse E, Yilmaz P, Gerken J, Schweer T, Yarza P, Peplies J, Glöckner FO**. 2013. The SILVA ribosomal RNA gene database project: improved data processing and web-based tools. *Nucl. Acids Res.* **41**(D1):D590-D596.
27. **R Core Team. 2021.** A language and environment for statistical computing (v.4.1.2). https://www.R-project.org/. Retrieved 11 December 2021. {Code and/or software.}
28. **Wickham H, Averick M, Bryan J, Chang W, McGowan LD, François R, Grolemund G, Hayes A, Henry L, Hester J, Kuhn M, Pedersen TL, Miller E, Bache SM, Müller K, Ooms J, Robinson D, Seidel DP, Spinu V, Takahashi K, Vaughan D, Wilke C, Woo K, Yutani H.** 2019. Welcome to the Tidyverse. *J Open Source Softw.* **4**:1686.

29. **Oksanen J, Blanchet FG, Friendly M, Kindt R, Legendre P, McGlinn D, Minchin PR, O'Hara RB, Simpson GL, Solymos P, Stevens MHH, Szoecs E, Wagner H.** 2020. Vegan: Community ecology package (v.2.5-7). https://CRAN.R-project.org/package=vegan. Retrieved 11 December 2021. {Code and/or software.}
30. **Paradis E, Schliep K.** 2019. Ape 5.0: An environment for modern phylogenetics and evolutionary analyses in R. *Bioinformatics.* **35**:526–528.
31. **McMurdie PJ, Holmes S.** 2013. phyloseq: An R package for reproducible interactive analysis and graphics of microbiome census data. *PLoS One.* **8**:e61217.
32. **Love MI, Huber W, Anders S.** 2014. Moderated estimation of fold change and dispersion for RNA-seq data with DESeq2. *Genome Biol.* **15**:550.
33. **Wickham H.** 2016. ggplot2: Elegant Graphics for Data Analysis. https://ggplot2.tidyverse.org. Retrieved 11 December 2021. {Code and/or software.}
34. **Arnold JB.** 2021. ggthemes: Extra Themes, Scales and Geoms for 'ggplot 2' (v.4.2.4). https://CRAN.R-project.org/package=ggthemes. Retrieved 11 December 2021. {Code and/or software.}
35. **Li D, Ching K, Hunt WJ.** 2021. Examination into the HI-SEAS IV built environment reveals differences in the microbial diversity and composition of plastic and wood surfaces. *UJEMI.* **26**:1-10.
36. **Naureen Z, Rehman NU, Hussain H, Hussain J, Gilani SA, Al Housni SK, Mabood F, Khan AL, Farooq S, Abbas G, Harrasi AA**. 2017. Exploring the Potentials of *Lysinibacillus sphaericus* ZA9 for Plant Growth Promotion and Biocontrol Activities against Phytopathogenic Fungi. *Front Microbiol*. **8**:1477.
37. **Marson J, Berto S, Mouser P, Baldwin H**. 2021. Association between Rosacea, Environmental Factors, and Facial Cutaneous Dysbiosis: A Pilot Study from the Largest National Festival of Twins. *SKIN.* **5**(5):487–495.
38. **Ofek M, Hadar Y, Minz D**. 2012. Ecology of root colonizing *Massilia* (Oxalobacteraceae). *PLoS One*. **7**(7):e40117.
39. **Eren AM, Sogin ML, Morrison HG, Vineis JH, Fisher JC, Newton RJ, McLellan SL**. 2015. A single genus in the gut microbiome reflects host preference and specificity. *ISME J*. **9**(1):90-100.
40. **Vaz-Moreira I, Nunes OC, Manaia CM**. 2011. Diversity and antibiotic resistance patterns of Sphingomonadaceae isolates from drinking water. *Appl Environ Microbiol*. **77**(16):5697-706.
41. **Allen TD, Lawson PA, Collins MD, Falsen E, Tanner RS**. 2006. *Cloacibacterium normanense* gen. nov., sp. nov., a novel bacterium in the family Flavobacteriaceae isolated from municipal wastewater. *Int J Syst Evol Microbiol*. **56**(Pt 6):1311-1316.
42. **Takai K, Inoue A, Horikoshi K**. 1999. *Thermaerobacter marianensis* gen. nov., sp. nov., an aerobic extremely thermophilic marine bacterium from the 11,000 m deep Mariana Trench. *Int J Syst Bacteriol*. **49**(Pt 2):619-628.
43. **Molari M, Janssen F, Vonnahme T, Wenzhöfer F, Boetius A**. 2020. Microbial communities associated with sediments and 2 polymetallic nodules of the Peru Basin. *Biogeosci Discuss*. https://doi.org/10.5194/bg-2020-11.
44. **DeLong EF**. 2021. Exploring Marine Planktonic Archaea: Then and Now. *Front Microbiol*. **11**:616086.
45. **Ramirez J, Guarner F, Bustos Fernandez L, Maruy A, Sdepanian VL, Cohen H**. 2020. Antibiotics as Major Disruptors of Gut Microbiota. *Front Cell Infect Microbiol*. **10**:572912.